

Infrared Laser Spectrum and Structure of Phosphoryl Chloride (CIPO) Formed at Ambient Temperature in the Gas Phase

I. S. Bell,[†] P. A. Hamilton,[‡] and P. B. Davies^{*,†}

Department of Chemistry, University of Cambridge, Lensfield Road, Cambridge, CB2 1EW, U.K., and
Department of Chemistry, Queen Mary & Westfield College, Mile End Road, London, E1 4NS, U.K.

Received: July 22, 1998

The infrared spectrum of the transient molecule phosphoryl chloride (CIPO) has been measured in the gas phase at room temperature using infrared diode laser absorption spectroscopy around 8 μm . The molecule was generated in a flow system either by adding molecular chlorine to a mixture of white phosphorus vapor and oxygen or by reacting atomic oxygen with phosphorus trichloride vapor. The infrared spectrum arises from the P–O stretching fundamental (ν_1) of CIPO. The band origin is determined as 1263.007 00(22) cm^{-1} , which is 5 cm^{-1} higher than the Ar matrix value and nearly 10 cm^{-1} lower than a recent low-resolution gas phase FTIR measurement. The rotational constants derived from the diode laser experiment, $A = 1.120$, $B = 0.151429(29)$, and $C = 0.133\ 236(23)$ cm^{-1} , are very close to those calculated from the density functional theory (B3LYP) structure of $R_{\text{Cl-P}} = 2.0958$ Å, $R_{\text{P-O}} = 1.4650$ Å, and $\angle\text{Cl-P-O} = 110.07^\circ$.

Introduction

In comparison with nitrosyl halides, relatively little is known about the molecular structure of the homologous phosphoryl halides in the gas phase. The present state of knowledge regarding these species is summarized in the thorough review of Binnewies and Schnöckel.¹ Until the present study, CIPO had been prepared at high temperatures either by reacting metallic silver with POCl_3 or by partial hydrolysis of PCl_3 above 700 K.^{2,3} Mass spectrometry, photoelectron spectroscopy, and, very recently, low-resolution FTIR have been used to confirm its existence in the gas phase.^{2,4,5} The molecule can also be isolated in an inert gas matrix by photolysis of PCl_3 and O_3 .⁶ The kinetics of the $\text{O} + \text{PCl}_3$ reaction has been studied by Jourdain et al.,⁷ using a discharge flow mass spectrometer system to determine a rate constant of $(3 \pm 0.5) \times 10^{-11}$ $\text{cm}^3 \text{mol}^{-1} \text{s}^{-1}$. Observation of the products provides qualitative evidence that the reaction mechanism is broadly similar to the better understood $\text{O} + \text{PH}_3$ reaction. The only experimental structural information obtained about the CIPO molecule to date is the condensed phase infrared fundamental frequencies at 489(vs), 308(w), and 1258(vs) cm^{-1} ,² and the FTIR vibrational bands at 1272.8 and 491.6 cm^{-1} .⁵ We now report a study of CIPO in the gas phase using Doppler-limited infrared laser absorption spectroscopy.

Experimental Section

The molecule was generated in a fast flow system which incorporated a multipass (White) cell, as described previously.^{8,9} Tunable infrared radiation from a diode laser traversed the 1 m long absorption cell up to 40 times. A small-amplitude 1.3 kHz modulating current was applied to the driving current of the diode laser, with the absorption signal detected at twice this frequency by a lock-in amplifier. Absolute calibration of the spectra was achieved by synchronously recording the accurately

measured lines of N_2O ,¹⁰ and of a confocal étalon (free spectral range 0.0098 cm^{-1}) for relative calibration. The estimated accuracy of line measurement was 0.001 cm^{-1} . The molecule was first detected by adding molecular chlorine to the chemiluminescent region of the low-pressure chain reaction between oxygen and white phosphorus vapor.⁸ A stronger source of CIPO was found to be the reaction of oxygen atoms with PCl_3 vapor. Atomic oxygen was generated by a 2450 MHz microwave discharge in a 5% O_2/Ar mixture in a side arm and mixed with PCl_3 in the absorption cell. Optimum total pressures were about 100 mTorr.

Results and Discussion

At the high resolution of diode laser spectroscopy, many lines were detected between 1240 and 1280 cm^{-1} , *i.e.*, centered on the matrix value (1258 cm^{-1}) for the P–O stretch of CIPO. It was easily shown by chemical substitution that the transient molecule responsible for these lines contained Cl, P, and O atoms, and the density of lines ruled out a carrier having symmetric top structure. Both chemical sources ($\text{P}_4 + \text{O} + \text{Cl}_2$ and $\text{O} + \text{PCl}_3$) provided identical spectra indicating that all the lines arose from a single species. For the vast majority of the spectra, there are no readily discernible patterns on the scale of the diode laser scans. A typical experimental spectrum is shown in Figure 1.

In order to simulate a rotationally resolved spectrum of CIPO and hence begin making an assignment, the structure of the molecule was first calculated using *ab initio* methods. Density functional theory (DFT) calculations using the B3LYP method were carried out with the Gaussian94 package and a variety of basis sets.¹¹ In addition to CIPO, identical calculations were carried out for the structurally analogous species SSO and ClNO, both of which have precisely determined experimental equilibrium geometries. The results are summarized in Table 1. In its ground electronic state, CIPO is nonlinear with a bond angle of about 110° . The *ab initio* structures of SSO and ClNO are compared directly with experiment in Table 1, and this enabled

* Corresponding author.

[†] University of Cambridge.

[‡] Queen Mary & Westfield College.

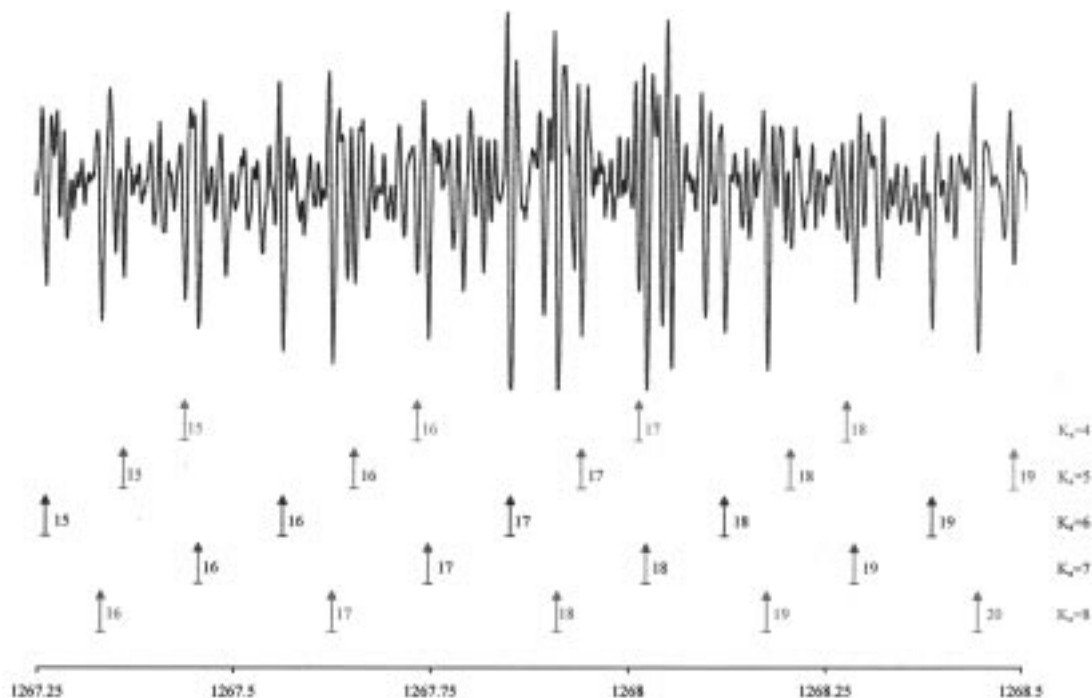


Figure 1. Typically congested region of the CIPO spectrum. A selected series of R-branch lines labeled according to their J assignment for different values of K_a are shown. Lines appear with second derivative line shape due to diode laser current modulation at 1.3 kHz and detection at 2.6 kHz.

TABLE 1: DFT Equilibrium Structures of CIPO, SSO, and CINO^a

	$R(X-Y)$	$R(Y-O)$	angle
CIPO			
6-31+G(d)	2.1102	1.4815	110.06
6-311+G(2d, p)	2.1139	1.4657	110.34
6-311+G(2df, 2p)	2.0958	1.4650	110.07
calcd rotational constants: ^b $A = 1.100 \text{ cm}^{-1}$, $B = 0.147 \text{ cm}^{-1}$, $C = 0.130 \text{ cm}^{-1}$			
scaled rotational constants: $A = 1.122 \text{ cm}^{-1}$, $B = 0.149 \text{ cm}^{-1}$, $C = 0.131 \text{ cm}^{-1}$			
SSO			
6-31+G(d)	1.9226	1.4892	117.56
6-311+G(2d, p)	1.9166	1.4701	118.03
6-311+G(2df, 2p)	1.9030	1.4662	117.74
expt (ref 12)	1.88424(11)	1.45621(13)	117.876(4)
CINO			
6-31+G(d)	1.9972	1.1429	114.09
6-311+G(2d, p)	2.0066	1.1292	114.21
6-311+G(2df, 2p)	1.9937	1.1285	114.23
expt (ref 13)	1.97453(25)	1.13354(25)	113.320(13)

^a Bond lengths are in Å, bond angles in deg. ^b Rotational constants of CIPO from the calculated structure at the 6-311+G(2df, 2p) level.

the results for CIPO to be scaled accordingly. In fact, this scaling had only a small effect on the parameters calculated with the largest basis set. The structure of CIPO is similar to SSO with a slightly more acute bond angle. All three molecules exhibited similar systematic changes in structure as the basis set was changed. The DFT structure of CIPO is similar to that obtained from the SCF, CI(SD), and CPF methods.¹ The calculated harmonic vibrational frequencies are presented in Table 2. There is good agreement between the calculated values and the observed band origins for SSO and CINO. The ν_1 band of CIPO is predicted to be relatively intense (Table 2) and to consist of a nearly pure P=O stretching motion. As a result of the small participation of the Cl atom in this vibration, the Cl isotopic shift for this band is calculated to be extremely small ($\sim 0.003 \text{ cm}^{-1}$).

From the calculated constants, the molecule is a near-prolate asymmetric top with Ray's asymmetry parameter¹⁶ $\kappa \approx -0.96$. The oscillating dipole along the P–O bond could give rise to both a-type (parallel) and b-type (perpendicular) bands. Both types of band were simulated using the rotational constants in Table 1 and Watson's A-reduced Hamiltonian.¹⁷ Very few simple spectral patterns were discernible in either simulation, in accord with the experimental spectra. Figure 2 shows the only recorded region with an apparently simple structure across the complete spectrum. It corresponds to the Q branches of an a-type (parallel) band for which $\Delta K_a = 0$, $\Delta J = 0$. Each line is an accumulation of unresolved J components for a particular value of K_a . The congestion of all the J components into a single spectral feature at such high resolution is clear evidence for a very small change in $\bar{B} = (B + C)/2$ on vibrational excitation. The splitting between successive K_a Q-branches for a molecule approaching the prolate top limit is given by the formula $2\Delta A(K_a + 1)$. The lines in Figure 2 fit this form almost perfectly to yield $\Delta A = -0.0079215(32) \text{ cm}^{-1}$. Fitting of the Q-branch structure also provides an unambiguous determination of the band centre as $1263.0052 \text{ cm}^{-1}$. The smaller satellite lines visible in the spectrum of Figure 2 arise from the less abundant ³⁷CIPO isotopomer. These lines may be similarly fitted to yield $\Delta A = -0.0079213(25) \text{ cm}^{-1}$ and a band center of $1262.9893 \text{ cm}^{-1}$ for the less abundant ³⁷CIPO species. The measured isotopic shift of 0.0159 cm^{-1} is in satisfactory agreement with the *ab initio* predictions.

Each K_a component of the Q-branch lies at the origin of its associated P- and R-branches. These are series of lines above and below each Q-branch with a spacing of approximately $2\bar{B}$, which commence at a frequency $\pm 2(K_a + 1)\bar{B}$ from the Q-branch line since $J \geq K_a$. The R-branch series were readily identified for $4 \leq K_a \leq 8$, leading to an accurate value for \bar{B} which was used to locate the P-branches. Figure 1 shows the assignment of the R-branch lines for several K_a values recorded in a single scan; many other lines, some assigned, are present in this spectrum. The selection rule for an a-type band of an

TABLE 2: Calculated Vibrational Band Origins^a

	ν_3	ν_2	ν_1	³⁷ Cl isotope shift ($\nu_{1(35)} - \nu_{1(37)}$)
		CIPO		
6-31+G(d)	295.13 (6.0)	480.39 (173)	1259.39 (129)	0.0028
6-311+G(2d, p)	294.90 (4.2)	478.80 (174)	1276.90 (122)	0.0032
6-311+G(2df, 2p)	301.70 (4.2)	486.10 (174)	1285.40 (121)	0.0037
expt (Ar matrix ²)	308 (w)	489 (vs)	1258 (vs)	
this work			1263.0070	
		SSO		
6-31+G(d)	371.07 (11.2)	664.12 (45.5)	1144.28 (169)	
6-311+G(2d, p)	376.09 (7.8)	668.55 (51.7)	1162.64 (178)	
6-311+G(2df, 2p)	381.47 (8.2)	682.25 (51.4)	1184.58 (178)	
expt (gas phase ¹²)		679.14	1166.45	
		CINO		
6-31+G(d)	329.19 (80.8)	609.49 (109)	1920.83 (655)	0.0573
6-311+G(2d, p)	332.19 (81.3)	607.28 (109)	1902.84 (672)	0.0604
6-311+G(2df, 2p)	333.03 (86.2)	610.46 (111)	1911.63 (671)	0.0657
expt (gas phase ^{14,15})	331.9	595.8	1799.74	0.1

^a The band centers are in cm^{-1} and refer to the ³⁵Cl isotopomer except where indicated. Calculated intensities are given in parentheses in units of km/mol .

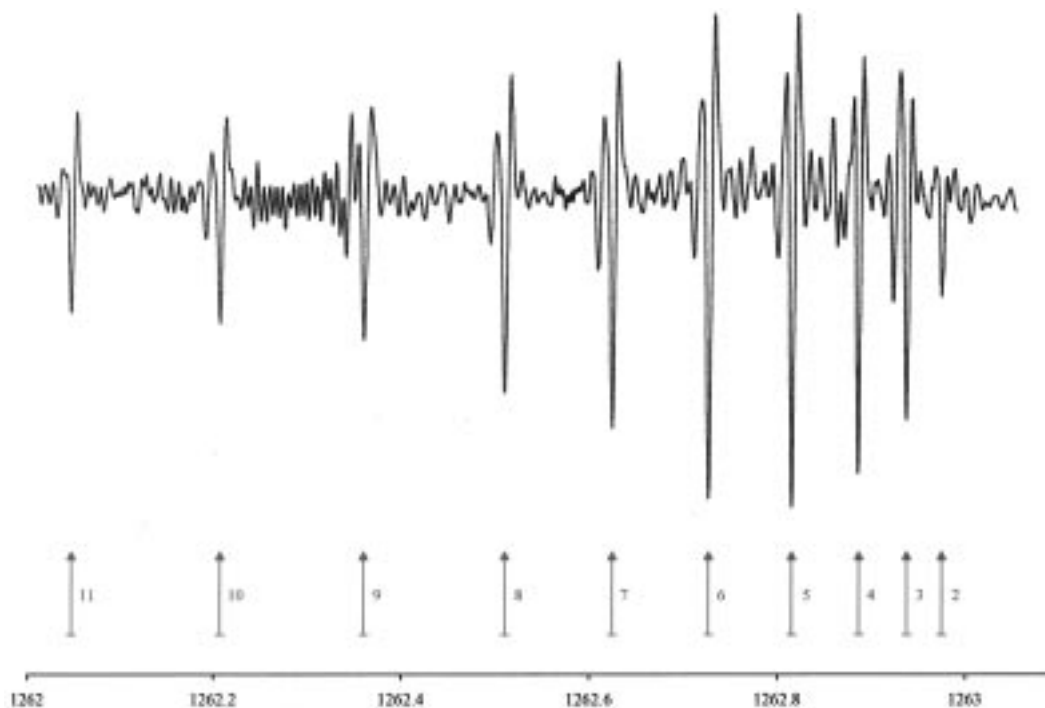


Figure 2. Diode laser absorption spectrum of the a-type Q-branch of the P–O stretch in CIPO. The lines are labeled according to the value of K_a and consist of unresolved J components.

asymmetric rotor means that the B and C constants can only be well determined individually by resolving the asymmetry doubling. This splitting is evident only for low K_a lines, and we have been able to resolve it for lines with $1 \leq K_a \leq 3$. Some 44 of the more intense asymmetry split lines have been assigned, so that the B and C constants are reasonably well determined in both states. The unambiguous assignment of the P- and R-branch lines for the ³⁷CIPO isotopomer has not been possible at this stage due to the heavy congestion of the spectra and the lower concentration of this species.

Although the ΔA value is well determined from this spectrum, the absolute value of A in each state cannot be determined from observation of only an a-type (parallel) band in the symmetric top limit, which CIPO approaches. Allowing A in both vibrational states to float in fits to the assigned lines thus generates large uncertainties, with a 1σ error in both A values of $\pm 0.02 \text{ cm}^{-1}$ and significantly increased uncertainty in the B

TABLE 3: Fitted Parameters (cm^{-1}) for the Ground and $\nu_3 = 1$ States of CIPO^a

	ground state	$\nu_3 = 1$ state
ν_0		1263.00700(22)
A	1.120 ^b	1.1120593(85)
B	0.151429(29)	0.151383(28)
C	0.133236(23)	0.133103(24)
Δ_J	$1.42(32) \times 10^{-7}$	$1.68(26) \times 10^{-7}$
Δ_{JK}	$-8.6(32) \times 10^{-7}$	$-10.1(28) \times 10^{-7}$
Δ_K^c	4.0×10^{-5}	4.0×10^{-5}
δ_J^c	1.1×10^{-8}	1.1×10^{-8}
δ_K^c	4.1×10^{-7}	4.1×10^{-7}

^a Quoted errors are 1σ in units of the last digit given. ^b Fixed at this value (see text). ^c The parameters Δ_K , δ_J , and δ_K could not be well determined and were therefore fixed at the SSO values for both vibrational states.

and C values. A better constraint on the ground state value of A can be achieved by assuming that the inertial defect in CIPO

TABLE 4: Observed Lines in the ν_3 Band of CIPO^a

lower state			upper state			obs	diff	lower state			upper state			obs	diff
<i>J</i>	<i>K_a</i>	<i>K_c</i>	<i>J</i>	<i>K_a</i>	<i>K_c</i>			<i>J</i>	<i>K_a</i>	<i>K_c</i>	<i>J</i>	<i>K_a</i>	<i>K_c</i>		
2	1	2	1	1	1	1262.4470	-8	9	5	5	8	5	4	1260.2410	1
3	1	3	2	1	2	1262.1703	-16	10	5	6	9	5	5	1259.9534	-8
5	1	5	4	1	4	1261.6184	-18	11	5	7	10	5	6	1259.6678	5
6	1	6	5	1	5	1261.3445	1	12	5	8	11	5	7	1259.3805	4
7	1	7	6	1	6	1261.0682	-6	13	5	9	12	5	8	1259.0920	-6
8	1	8	7	1	7	1260.7932	0	14	5	10	13	5	9	1258.8052	3
9	1	9	8	1	8	1260.5190	11	7	6	1	6	6	0	1260.7272	0
10	1	10	9	1	9	1260.2412	-16	8	6	2	7	6	1	1260.4407	-4
11	1	11	10	1	10	1259.9672	-6	9	6	3	8	6	2	1260.1561	13
12	1	12	11	1	11	1259.6930	-1	10	6	4	9	6	3	1259.8695	12
13	1	13	12	1	12	1259.4199	13	11	6	5	10	6	4	1259.5814	-2
14	1	14	13	1	13	1259.1441	-1	12	6	6	11	6	5	1259.2936	-11
3	2	1	2	2	0	1262.1216	15	13	6	7	12	6	6	1259.0084	10
5	2	3	4	2	2	1261.5468	7	14	6	8	13	6	7	1258.7225	25
6	2	4	5	2	3	1261.2571	-4	15	6	9	14	6	8	1258.4332	10
7	2	5	6	2	4	1260.9675	0	16	6	10	15	6	9	1258.1435	-7
8	2	6	7	2	5	1260.6766	4	2	2	0	2	2	1	1262.9745	-3
3	2	2	2	2	1	1262.1216	5	3	3	0	3	3	1	1262.9341	-12
4	2	3	3	2	2	1261.8367	6	4	4	0	4	4	1	1262.8790	-6
6	2	5	5	2	4	1261.2665	4	5	5	0	5	5	1	1262.8073	-8
8	2	7	7	2	6	1260.6979	14	5	5	1	5	5	0	1262.8073	-8
9	2	8	8	2	7	1260.4121	2	6	6	0	6	6	1	1262.7196	-12
10	2	9	9	2	8	1260.1271	-4	6	6	1	6	6	0	1262.7196	-12
11	2	10	10	2	9	1259.8427	-5	7	6	1	7	6	2	1262.7196	0
12	2	11	11	2	10	1259.5602	9	7	6	2	7	6	1	1262.7196	0
13	2	12	12	2	11	1259.2737	-18	7	7	0	7	7	1	1262.6160	-16
14	2	13	13	2	12	1258.9932	11	8	8	0	8	8	1	1262.4974	-13
15	2	14	14	2	13	1258.7096	6	9	9	0	9	9	1	1262.3630	-9
16	2	15	15	2	14	1258.4271	9	10	10	0	10	10	1	1262.2134	0
17	2	16	16	2	15	1258.1435	-3	11	11	0	11	11	1	1262.0478	6
5	4	1	4	4	0	1261.4572	15	2	2	1	3	2	2	1263.8309	24
6	4	2	5	4	1	1261.1705	6	3	2	2	4	2	3	1264.1145	22
7	4	3	6	4	2	1260.8837	-1	4	2	3	5	2	4	1264.3972	16
8	4	4	7	4	3	1260.5978	3	5	2	4	6	2	5	1264.6798	12
9	4	5	8	4	4	1260.3115	7	6	2	5	7	2	6	1264.9606	-4
10	4	6	9	4	5	1260.0240	1	9	2	8	10	2	9	1265.8049	-1
11	4	7	10	4	6	1259.7356	-10	10	2	9	11	2	10	1266.0840	-10
12	4	8	11	4	7	1259.4480	-10	11	2	10	12	2	11	1266.3637	-5
13	4	9	12	4	8	1259.1608	-2	12	2	11	13	2	12	1266.6424	-2
14	4	10	13	4	9	1258.8719	-7	13	2	12	14	2	13	1266.9208	7
15	4	11	14	4	10	1258.5811	-27	14	2	13	15	2	14	1267.1950	-18
6	5	2	5	5	1	1261.0989	-5	15	2	14	16	2	15	1267.4711	-13
7	5	3	6	5	2	1260.8127	-7	17	2	16	18	2	17	1268.0208	2
8	5	4	7	5	3	1260.5287	14	18	2	17	19	2	18	1268.2942	12
3	3	0	4	3	1	1264.0747	9	16	5	11	17	5	12	1267.6296	0
4	3	1	5	3	2	1264.3573	-6	17	5	12	18	5	13	1267.9149	29
5	3	2	6	3	3	1264.6420	-1	18	5	13	19	5	14	1268.1951	8
6	3	3	7	3	4	1264.9273	11	19	5	14	20	5	15	1268.4767	2
7	3	4	8	3	5	1265.2084	-21	6	6	1	7	6	2	1264.7145	13
8	3	5	9	3	6	1265.4945	-4	7	6	2	8	6	3	1264.9960	-7
9	3	6	10	3	7	1265.7779	-17	8	6	3	9	6	4	1265.2814	14
10	3	7	11	3	8	1266.0635	-10	9	6	4	10	6	5	1265.5638	6
11	3	8	12	3	9	1266.3509	10	10	6	5	11	6	6	1265.8464	1
13	3	10	14	3	11	1266.9212	-10	11	6	6	12	6	7	1266.1295	3
14	3	11	15	3	12	1267.2086	-9	12	6	7	13	6	8	1266.4120	1
15	3	12	16	3	13	1267.4977	1	13	6	8	14	6	9	1266.6949	4
16	3	13	17	3	14	1267.7870	3	14	6	9	15	6	10	1266.9779	10
17	3	14	18	3	15	1268.0781	11	15	6	10	16	6	11	1267.2596	5
18	3	15	19	3	16	1268.3685	1	16	6	11	17	6	12	1267.5405	-6
4	4	0	5	4	1	1264.3028	1	17	6	12	18	6	13	1267.8231	1
5	4	1	6	4	2	1264.5866	0	18	6	13	19	6	14	1268.1036	-11
6	4	2	7	4	3	1264.8701	-3	19	6	14	20	6	15	1268.3880	18
7	4	3	8	4	4	1265.1533	-8	7	7	0	8	7	1	1264.8931	-17
8	4	4	9	4	5	1265.4392	15	8	7	1	9	7	2	1265.1777	-4
9	4	5	10	4	6	1265.7209	-4	9	7	2	10	7	3	1265.4624	11
10	4	6	11	4	7	1266.0038	-10	10	7	3	11	7	4	1265.7450	7
11	4	7	12	4	8	1266.2880	-3	11	7	4	12	7	5	1266.0274	3
12	4	8	13	4	9	1266.5720	2	12	7	5	13	7	6	1266.3109	12
13	4	9	14	4	10	1266.8550	-3	13	7	6	14	7	7	1266.5917	-5
14	4	10	15	4	11	1267.1384	-4	14	7	7	15	7	8	1266.8743	-1
15	4	11	16	4	12	1267.4212	-12	15	7	8	16	7	9	1267.1555	-10
16	4	12	17	4	13	1267.7055	-5	16	7	9	17	7	10	1267.4381	-2

TABLE 4 (Continued)

lower state			upper state			obs	diff	lower state			upper state			obs	diff
<i>J</i>	<i>K_a</i>	<i>K_c</i>	<i>J</i>	<i>K_a</i>	<i>K_c</i>			<i>J</i>	<i>K_a</i>	<i>K_c</i>	<i>J</i>	<i>K_a</i>	<i>K_c</i>		
17	4	13	18	4	14	1267.9895	-3	17	7	10	18	7	11	1267.7196	-4
18	4	14	19	4	15	1268.2716	-21	18	7	11	19	7	12	1268.0005	-9
18	4	15	19	4	16	1268.2716	9	19	7	12	20	7	13	1268.2823	-3
6	5	1	7	5	2	1264.7995	0	10	8	3	11	8	4	1265.6276	8
7	5	2	8	5	3	1265.0820	-11	11	8	4	12	8	5	1265.9092	-4
8	5	3	9	5	4	1265.3680	15	12	8	5	13	8	6	1266.1933	11
9	5	4	10	5	5	1265.6493	-5	13	8	6	14	8	7	1266.4747	1
10	5	5	11	5	6	1265.9328	-2	14	8	7	15	8	8	1266.7562	-6
11	5	6	12	5	7	1266.2161	0	15	8	8	16	8	9	1267.0385	-3
12	5	7	13	5	8	1266.4989	-1	16	8	9	17	8	10	1267.3214	8
13	5	8	14	5	9	1266.7823	5	17	8	10	18	8	11	1267.6033	12
14	5	9	15	5	10	1267.0663	17	18	8	11	19	8	12	1267.8840	6
15	5	10	16	5	11	1267.3481	9	19	8	12	20	8	13	1268.1628	-17

^a Obs is the observed transition frequency in cm⁻¹. Diff is the observed value minus the calculated value, in units of 10⁻⁴ cm⁻¹.

is similar to that in ClNO and SSO. These two molecules have similar small positive inertial defects of 0.139 and 0.176 amu Å², respectively, and a value of 0.15 amu Å² was therefore adopted as reasonable for ClPO. As *B* and *C* are virtually independent of *A*, the ground state *A* value can be iteratively refined to provide a consistent set of ground state constants which both fit the observed data and give this inertial defect. The values of all the constants determined by this method are slightly dependent on the adopted ground state *A* value, and therefore may be subject to small changes when an accurate value of *A* becomes known. Eventually over 170 lines were assigned (about 40% of the total observed) and fitted with a root mean square deviation of 0.000 97 cm⁻¹ to yield the parameters in Table 3. The full list of observed transitions, along with deviations from the calculated values, is given in Table 4.

The gas phase ν_3 band origin is blue shifted by 5 cm⁻¹ with respect to the Ar matrix value. The magnitude of the shift is entirely reasonable in comparison with the blue shift in other P—O stretching frequencies, *e.g.* in PO (2.5 cm⁻¹) and P₂O (ν_3 , 7.2 cm⁻¹). The vibrational band center is also in excellent agreement with the *ab initio* results. The very small isotopic shift observed confirms the *ab initio* prediction that the vibration is a nearly pure P=O stretching motion. The rotational parameters determined show close agreement with the DFT values for the *B* and *C* constants, confirming the calculated structure. The 10 cm⁻¹ difference in the band origin in comparison with the FTIR study may be due to the low resolution of the recording. Certainly no obvious Q-branch was found at 1272.8 cm⁻¹ as reported by Allaf and Boustani.

Conclusions

At present, we have not been able to identify obvious features from a b-type (perpendicular) band but many lines remain to be assigned in the spectrum. The present spectroscopic results confirm the structure and bonding of ClPO deduced from high-level *ab initio* calculations. These constants should enable searches to be made for the microwave spectrum of ClPO, which should be reasonably intense (calculated dipole moments $\mu_b = 1.94$ D, $\mu_a = 0.33$ D). The detection of ClPO with good signal

to noise ratios suggests that many other homologues of the nitrosyl and thionitrosyl halides may be formed and detected by this technique.

Acknowledgment. We are grateful to Dr. B. J. Howard of Oxford University for the loan of a diode laser, and to Unilever Research, Port Sunlight Laboratory, for an equipment grant. I.S.B. acknowledges financial support from the EPSRC, Schlumberger Cambridge Research, and the Isaac Newton Trust.

References and Notes

- (1) Binnewies, M.; Schnöckel, H. *Chem. Rev.* **1990**, *90*, 321.
- (2) Binnewies, M.; Lakenbrink, M.; Schnöckel, H. *Z. Anorg. Allg. Chem.* **1983**, *497*, 7.
- (3) Schnöckel, H. Schunck, H. *Z. Anorg. Allg. Chem.* **1987**, *548*, 161.
- (4) Binnewies, M.; Solouki, B.; Bock, H.; Becherer, R.; Ahlrichs, R. *Angew. Chem., Int. Ed. Engl.* **1984**, *23*, 731.
- (5) Allaf, A. W.; Boustani, I. *Vib. Spectrosc.* **1998**, *16*, 69.
- (6) Moores, B. W.; Andrews, L. *J. Phys. Chem.* **1989**, *93*, 1902.
- (7) Jourdain, J.-L.; Laverdet, G.; Lebras, G.; Combourieu, J. *J. Chem. Phys.* **1980**, *77*, 809.
- (8) Bell, I. S.; Qian, H.-B.; Hamilton, P. A.; Davies, P. B. *J. Chem. Phys.* **1997**, *107*, 8311.
- (9) Bell, I. S.; Hamilton, P. A.; Davies, P. B. *Mol. Phys.* **1998**, *94*, 685.
- (10) Maki, A. G.; Wells, J. S. *Wavenumber Calibration Tables from Heterodyne Frequency Measurements*; NIST Special Publication 821; U.S. Government Printing Office, Washington, DC, 1991.
- (11) Frisch, M. J.; Trucks, G. W.; Schlegel, H. B.; Gill, P. M. W.; Johnson, B. G.; Robb, M. A.; Cheeseman, J. R.; Keith, T.; Petersson, G. A.; Montgomery, J. A.; Raghavachari, K.; Al-Laham, M. A.; Zakrzewski, V. G.; Ortiz, J. V.; Foresman, J. B.; Cioslowski, J.; Stefanov, B. B.; Nanayakkara, A.; Challacombe, M.; Peng, C. Y.; Ayala, P. Y.; Chen, W.; Wong, M. W.; Andres, J. L.; Replogle, E. S.; Gomperts, R.; Martin, R. L.; Fox, D. J.; Binkley, J. S.; Defrees, D. J.; Baker, J.; Stewart, J. P.; Head-Gordon, M.; Gonzalez, C.; Pople, J. A. *Gaussian 94, Revision D.3*; Gaussian Inc.: Pittsburgh, PA, 1995.
- (12) Lindenmayer, J.; Rudolph, H. D.; Jones, H. *J. Mol. Spectrosc.* **1986**, *119*, 56.
- (13) Cazzoli, G.; Degli Esposti, C.; Palmieri, P.; Simeone, G. *J. Mol. Spectrosc.* **1983**, *97*, 165.
- (14) Jones, L. H.; Ryan, R. R.; Asprey, L. B. *J. Chem. Phys.* **1967**, *49*, 581.
- (15) Chiekh, M.; Alamichel, C.; Chevillard, J. P.; Hubbard, R. *Chem. Phys. Lett.* **1986**, *125*, 283.
- (16) Kroto, H. W. *Molecular Rotation Spectra*; Dover: New York, 1992; p 41.
- (17) Watson, J. K. G. In *Vibrational Spectra and Structure*; Durig, J. R., Ed.; Elsevier: Amsterdam, 1977; Vol. 6, pp 1–89.